Spectral Characterization using Continuous Functions

Tomasz J. Cholewo and Steven F. Weed
Lexmark International, Inc., Lexington, KY, USA
e-mail: cholewo@lexmark.com

Abstract

Spectral characterization is often performed based on the set of measured spectral color signals and corresponding scalar sensor responses. Most methods attempt to reconstruct the sensor sensitivities at a discrete set of specific wavelengths or as a linear combination of basis functions. This paper describes a general method for estimating spectra using a direct regression of the discrete data with a continuous function by means of nonlinear optimization of its parameters. A priori information such as positivity and smoothness constraints and other assumed physical properties of the sensor are incorporated in the estimation process by an appropriate choice of the function. Results are provided for a simple neural network approximator which can be used for modeling of a wide variety of spectral functions. The proposed method is compared with quadratic programming, pseudoinverse, principal eigenvectors, and direct physical measurements.

Introduction

Spectral characterization attempts to estimate sensor sensitivity using sensor responses to known spectral color signals and additional a priori information. It is an active field of research and there are many published methods: pseudoinverse and principal eigenvector methods [1], SVD with Tikhonov regularization [2], Wiener estimation [3], projection onto convex sets [1], linear programming [4], and quadratic programming [5, 6]. These methods try to directly reconstruct the sensitivity spectra as sets of unrelated values for specific wavelengths or linear combinations of basis functions.

Alternatively, a predetermined parameterized nonlinear function can be regressed directly to pairs of reflectance spectra and sensor responses. Skewed and kurtosed Gaussian functions used in [7] can work well for CCD sensitivities but are less appropriate for estimation of illuminants or total scanner response. In the general case, minimizing a regression error function requires use of nonlinear optimization methods. In this paper a general analytical method for computation of the error function gradient is presented. It allows efficient use of an arbitrary continuous function to approximate the relationship between a wavelength and a response such as sensor sensitivity or illuminant spectral power distribution (SPD). A non-parametric model such as a neural network does not require a priori assumptions about a specific functional form of the spectral sensitivity.

The Characterization Approach

An approximation of sensor response $\hat{t}_i$ to spectral reflectance $r_i(\lambda)$ of the test patch i can be modeled as

$$\hat{t}_i(\boldsymbol{w}) = \int_{-\infty}^{\infty} m(\lambda, \boldsymbol{w}) r_i(\lambda) d\lambda \tag{1}$$

where $m(\lambda, \boldsymbol{w})$ is a continuous function of the wavelength λ characterized by a vector of p parameters $\boldsymbol{w} = [w_1, \ldots, w_p]$. In this formulation it is assumed that the illuminant is not known a priori and m incorporates effects of the illuminant, filter transmittance, and detector sensitivity. However, this equation can be also applied when an illuminant is known by pre-multiplying $r_i(\lambda)$ by the spectral power distribution of this illuminant.

We propose a method for estimating m by direct fitting to experimental data. First we define the estimation error for patch i

$$e_i(\boldsymbol{w}) = \hat{t}_i(\boldsymbol{w}) - t_i$$

where t_i is the actual (possibly linearized) sensor response for patch i. The total error function is expressed as a sum of squares of the individual patch errors:

$$E(\boldsymbol{w}) = \frac{1}{2} \sum_i e_i^2(\boldsymbol{w}).$$

The parameters producing the best least-squares fit of the function to the sensitivity of the sensor are obtained by minimizing the error criterion:

$$\boldsymbol{w}^* = \arg\min_{\boldsymbol{w}} E(\boldsymbol{w}). \tag{2}$$

Additional a priori requirements are most easily accommodated by choosing a specific functional form for m. If additional constraints are needed they can be added to Equation (2) as additional error penalty terms or as constraints to form a nonlinear programming problem. Figure 1 shows the simplified diagram of the estimation process.

The best-fit parameters $\boldsymbol{w}$ can be found using any nonlinear optimization algorithm. One of the simplest is gradient

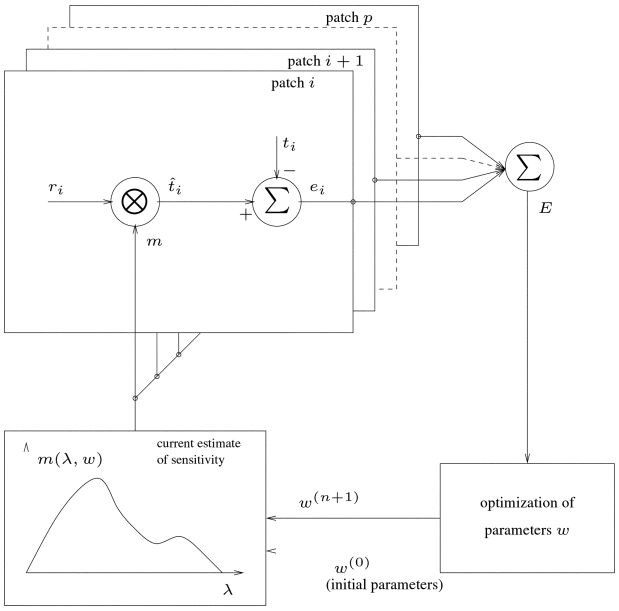

Figure 1. Block diagram of the iterative optimization process.

descent, where the parameters w are iteratively modified by a fraction α of the negative gradient of the error function until a proximity of the minimum is reached:

$$\boldsymbol{w}^{(n+1)} = \boldsymbol{w}^{(n)} - \alpha \nabla_{\boldsymbol{w}} E(\boldsymbol{w}).$$

This paper employs a more advanced second-order algorithm known as Scaled Conjugate Gradient [8] which significantly improves the speed and convergence of optimization.

The error gradient is a vector of partial derivatives of the error function with respect to each of the parameters w_k:

$$\nabla_{\boldsymbol{w}} E(\boldsymbol{w}) = \left[\frac{\partial E}{\partial w_1}, \ldots, \frac{\partial E}{\partial w_p} \right].$$

Components of the gradient can be computed from the chain rule:

$$\begin{aligned} \frac{\partial E(\boldsymbol{w})}{\partial w_k} &= \sum_i e_i(\boldsymbol{w}) \frac{\partial e_i(\boldsymbol{w})}{\partial w_k} \\ &= \sum_i e_i(\boldsymbol{w}) \frac{\partial \hat{t}_i(\boldsymbol{w})}{\partial w_k} \\ &= \sum_i e_i(\boldsymbol{w}) \int_{-\infty}^{\infty} \frac{\partial m(\lambda, \boldsymbol{w})}{\partial w_k} r_i(\lambda) d\lambda \end{aligned} \tag{3}$$

without resorting to finite-difference approximations.

In practice, the measurements of test patch reflectances are done at a limited and discrete set of wavelengths [9], for example, at 31 points from 400 nm to 700 nm with 10 nm spacing. Then the integrals in Equations (1) and (3) can be replaced with sums:

$$\hat{t}_i(\boldsymbol{w}) = \sum_{\lambda} m(\lambda, \boldsymbol{w}) r_i(\lambda)$$

and

$$\frac{\partial E(\boldsymbol{w})}{\partial w_k} = \sum_i e_i(\boldsymbol{w}) \sum_{\lambda} \frac{\partial m(\lambda, \boldsymbol{w})}{\partial w_k} r_i(\lambda).$$

In a trivial case, function *m* can be just a lookup table with each of the parameters w_λ simply storing the response for a wavelength λ:

$$m(\lambda, \boldsymbol{w}) = \sum_k w_k \delta(\lambda - \lambda_k)$$

where

$$\delta(\lambda - \lambda_k) = \begin{cases} 1 & \text{if} \quad \lambda = \lambda_k; \\ 0 & \text{otherwise.} \end{cases}$$

Then, from Equation (3), the derivative

$$\frac{\partial m(\lambda, \boldsymbol{w})}{\partial w_k} = \delta(\lambda - \lambda_k)$$

and, from Equation (1),

$$\hat{t}_i(\boldsymbol{w}) = \sum_{\lambda} w_\lambda r_i(\lambda).$$

In vector notation:

$$\boldsymbol{t} = \boldsymbol{R}\boldsymbol{w}$$

where *t* is a column vector of sensor responses for each test patch and ***R*** is a matrix with each row describing the spectral reflectance of each patch. The optimization problem from Equation (2) then becomes

$$\boldsymbol{w}^* = \arg\min_{\boldsymbol{w}} \left[\frac{1}{2} (\boldsymbol{R}\boldsymbol{w} - \boldsymbol{t})^2 \right]. \tag{4}$$

Equation (4) can be solved in the least squares sense without resorting to nonlinear optimization algorithms by the well-known pseudoinverse (PI) method [1]

$$\boldsymbol{w} = \boldsymbol{R}^{\dagger}\boldsymbol{t} \tag{5}$$

where symbol † denotes Moore-Penrose matrix inverse. This shows that for a specific formulation of *m* our method is identical to the pseudoinverse algorithm.

The matrix of real-object reflectance spectra ***R*** is highly ill-conditioned and contains only seven to eight significant singular values [10]. Its pseudoinverse is very sensitive to noise. This motivates the principal eigenvectors (PE) algorithm, also known as rank-deficient pseudoinverse [1]. It retains only the eigenvectors corresponding to the n largest singular values from the SVD decomposition of matrix ***R***. The pseudoinverse is a special case of the principal eigenvectors method where all 31 eigenvectors (for the case of 31 spectrum samples) are employed. Unfortunately, PE is still very

vulnerable to noise while giving worse results than PI for low noise data. These problems manifest themselves with undesired features such as negative and discontinuous sensitivities for some wavelengths.

Most of these problems can be avoided by adding additional constraints on the pseudoinverse solution ([4, 5]). Quadratic programming allows solving of Equation (5) in the least squares sense subject to conditions enforcing smoothness and positivity of the result. In our experiments we used QLD algorithm [11] with smoothness constraint

$$|1/4\, w_{i-1} - 1/2\, w_i + 1/4\, w_{i+1}| < \epsilon.$$

The results are labeled with symbol QP. We also used QP with the additional positivity and boundedness constraint of the form $0 \leq w_i \leq 1$ and labeled the results as QP+. Another way of enforcing smoothness is by adding a weighted regularization term to the error function [6].

There is usually no need to evaluate the resulting function at wavelengths not present in the initial measurement set. Any continuous function passing through the same points will produce identical results when used in the approximate discrete spectral calculations. The quality of the interpolation between these wavelengths is related to the generalization capabilities of the curve family employed.

Spectral sensitivity estimation is usually done independently for each channel unless there is a priori knowledge that the sensor signals are not actually independent. In a common case, when an internal 3×3 matrix is used to improve color fidelity of the device, a vector-valued function m with three-dimensional values (for example a neural network with an additional layer having three linear outputs) could be employed to separate the signals simultaneously while estimating the sensitivities.

Results

Publication IEC 61966-8 [4] is an international standard concerned with calibration and evaluation of scanners. It recommends a linear programming method to estimate the scanner sensor sensitivities using scans and spectral measurements of a test chart shown in Figure 2 containing a wide range of spectral reflectances from a population of relatively pure real print colorants (Figure 3). Singular value analysis indicates that spectra of this chart have higher intrinsic dimensionality than GretagMacbeth's ColorChecker, justifying a model with more parameters.

A series of experiments compared the proposed method with other approaches. As an approximating function we chose a simple single input (wavelength), a single hidden layer with N_h neurons, and a single-output (sensor response) neural network. The explicit functional form was:

$$m(\lambda, \boldsymbol{w}) = \frac{1}{2}\big(1+\tanh\big[w_1+\sum_{h=1}^{N_h} w_{tp}\tanh(w_p+\lambda w_{p\lambda})\big]\big).$$

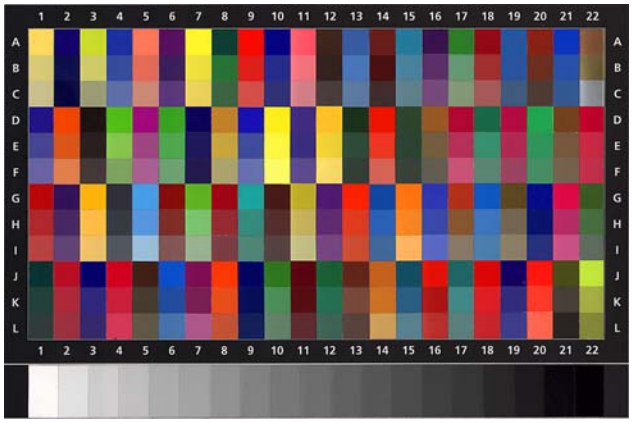

Figure 2: IEC *61966-8 test chart.*

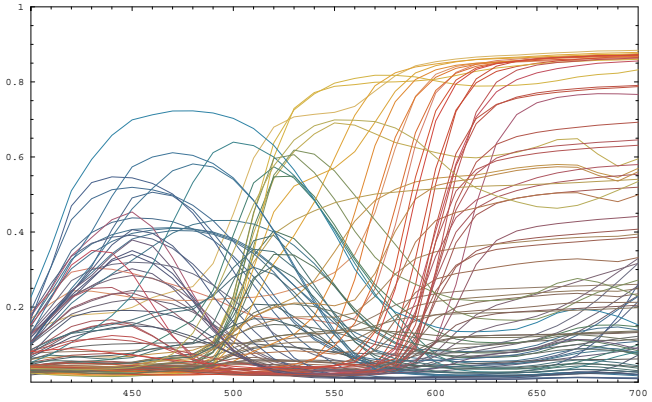

Figure 3: *Reflectance spectra of the 88 most chromatic patches from the* IEC *61966-8 chart (rows A, D, G, and J).*

The resulting function is nonlinear with respect to all its parameters. Since the $\tanh(\cdot)$ function range is $[-1, 1]$, the output of m is limited to $[0, 1]$. It provides a simple way of enforcing both the positivity and limited amplitude constraints though it may require pre-scaling the data to make sure that no valid sensitivities are larger than 1.

The estimation process is started either with random initial parameters $\boldsymbol{w}^{(0)}$ or, if a good initial sensitivity curve form is known, with a set of parameters corresponding to this curve.

Our first experiment attempted to estimate the CIE color matching functions (Figure 4a) from the spectral measurements of the IEC 61966-8 chart and the corresponding ideal computed XYZ values with varying levels of Gaussian noise. Synthetic data allows full control over the noise. Spectral measurements were pre-multiplied by the known power distribution of illuminant D50. RMS errors in estimates from neural networks with 20 hidden neurons (model NN(20)) are compared to pseudoinverse (PI and PI+), quadratic programming (QP and QP+), and PE with 7 most significant singular values (Figure 4b). The RMS errors in PE results approach

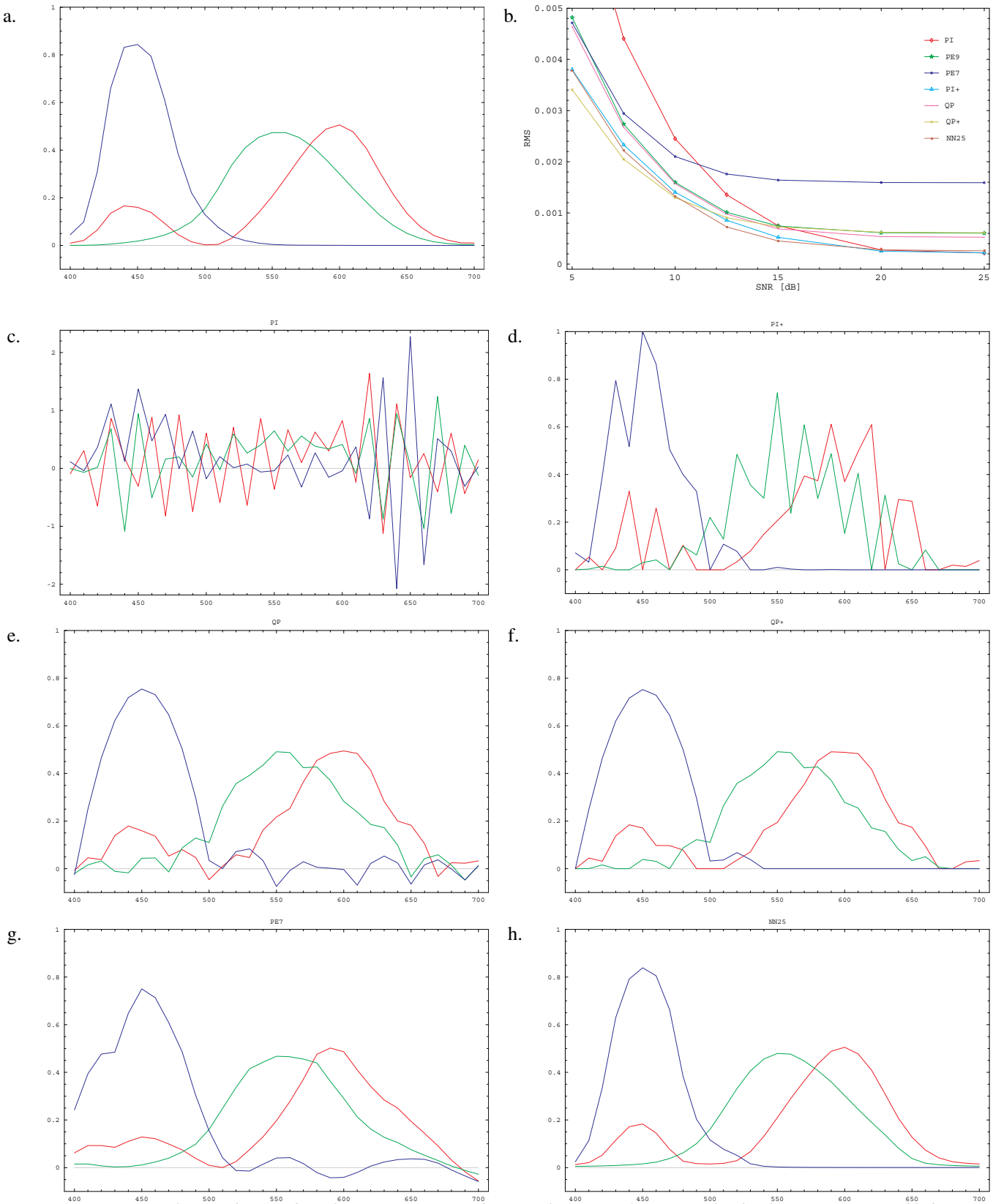

Figure 4: Estimation of CIE *color matching functions: a. target; b.* RMS *of estimates for varying levels of Gaussian noise added to* XYZ *values. Estimates for 20 dB* SNR *Gaussian noise: c.* PI*; d.* PI+*; e.* QP*; f.* QP+*; g.* PE(7)*; h.* NN(25).

zero as the number of singular values approaches the number of spectrum samples, but these solutions have infeasible spectral responses (Figure 4c,e). RMS results for neural networks are competitive with pseudoinverse, with spectral responses (Figure 4h) that agreeably approximate their targets.

A second experiment estimated the power distribution of illuminant D50 from reflectance spectra pre-multiplied with the CIE color matching function. The relative power distribution (CIE standard specifies illuminants in terms of an arbitrary unit of radiant power [12]) was scaled to the $[0, 1]$ range as shown in Figure 5a. The assumed sensor outputs t_i were XYZ values with Gaussian noise. Results (Figure 5b–f) demonstrate that despite low RMS values, sharp spikes in the illuminant SPD are difficult to reproduce. Likely reasons are that the IEC chart reflectances do not have sufficiently sharp transitions and that the added noise forces the least squares fit to find a middle, smooth approximation. Figure 6 shows estimation results obtained for illuminant F11 which is representative of tri-phosphor fluorescent lamps commonly used in desktop scanners.

Additional experiments were performed using spectral data measured for each patch of the IEC-61966-8 chart and the corresponding averages of RGB values from an image obtained with an Avision AV810C desktop scanner. The difficulty of direct measurements was actually one of the motivations for spectral reconstruction approaches. Spectral sensitivity capture was expedited by writing a custom application which combined monochromator (Optometrics' Scanning Digital Variable Wavelength Fiber Optic Module) and scanner driver control to handle repeated scans of a fiber bundle output. Monochromator and scanner lamp were calibrated using Ocean Optics USB 2000 spectrometer. Marginal signal-to-noise ratio for blue wavelengths is still a remaining measurement challenge and leads to large errors in this part of the spectrum.

Assuming that the sensor's response based on its physical properties should be proportional to the incident light, sensor characterization should be preceded by linearization of its luminance response. The achromatic patches at the bottom of the IEC chart were used to develop appropriate fourth degree polynomial fits.

Figure 7 compares measurements with estimates of actual scanner sensor responses combining sensor sensitivity, filter transmittance, and recording illumination. Scanner sensor spectral sensitivities were measured directly with nominal 2 nm resolution and lamp SPD was measured with nominal 0.2 nm resolution. Estimates were based on reflectances with 20 nm bandwidths. Approximating lower resolution estimates by triangular filters yields roughly comparable results, allowing for quantizing artifacts.

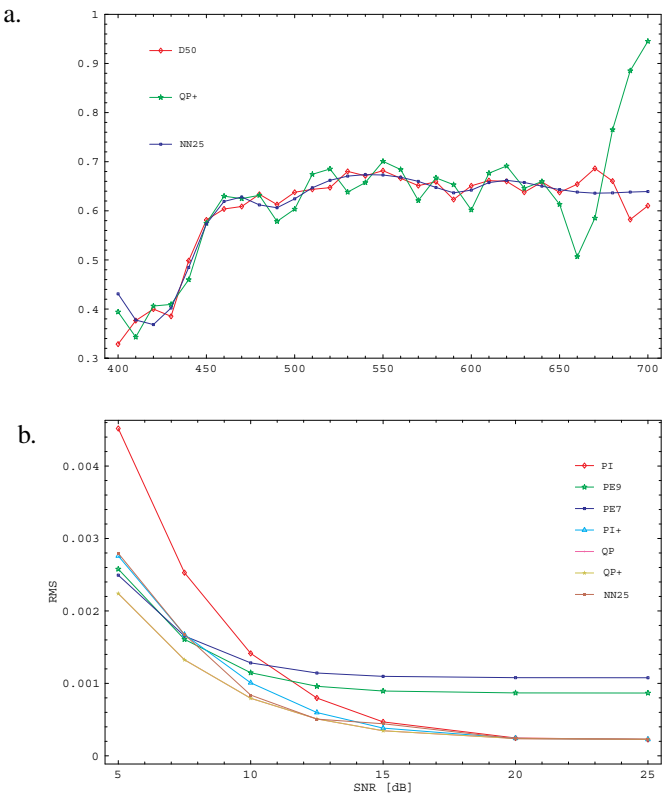

Figure 5: *Estimation of* CIE *illuminant D50 power distribution: a.* QP+ *and* NN(25) *estimates for 20 dB* SNR *Gaussian noise; b.* RMS *of estimates for varying levels of Gaussian noise added to* XYZ *values.*

Conclusions

Spectral device characterization rarely can replace empirical characterization performed for specific media and scene illumination but provides valuable insights into system design issues such as filter quality factors and metamerism. Consequently, it is interesting to contemplate robust approaches which treat the capture process approximately as a black box but still allow optimization of spectral design parameters.

Selecting an appropriate complexity for the approximating function is an important issue. Use of fewer parameters results in smoother solutions but increases risk of systematic bias resulting from the inability of the function to model the underlying phenomenon. On the other hand, too many parameters cause the function to exhibit large variance in response to irrelevant uncertainty and measurement noise, and the generalization will suffer. (Variance of even very large models can be controlled by means of regularization.) One possible solution is to divide available data into three sets: training, validation, and test. A whole range of estimates can be computed for varying function complexity using only the training set and one with the smallest error on the validation

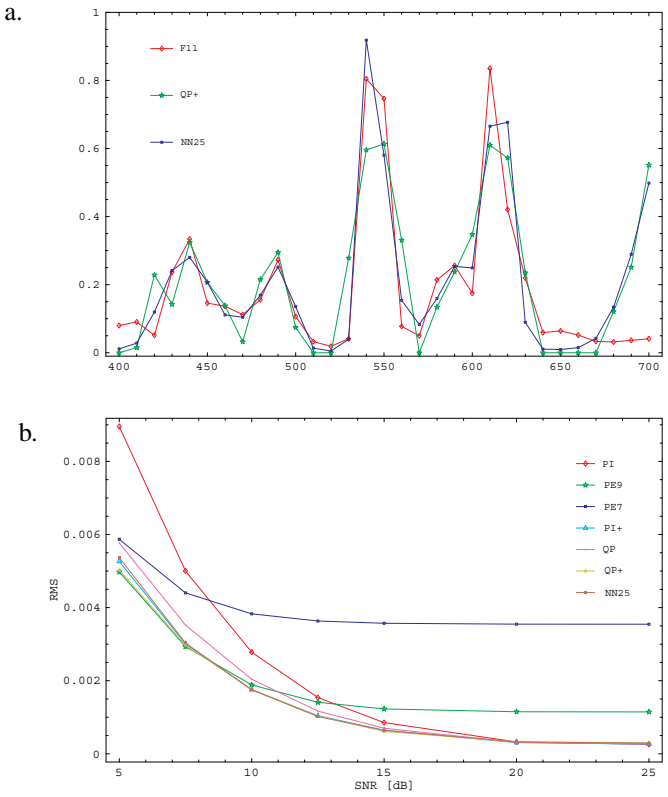

Figure 6: *Estimation of* CIE *illuminant F11 power distribution: a.* QP+ *and* NN(25) *estimates for 20 dB* SNR *Gaussian noise; b.* RMS *of estimates for varying levels of Gaussian noise added to* XYZ *values.*

set can be chosen. Finally, the withheld test set can be used to obtain an unbiased measure of the actual performance of the model.

While existing PI and PE methods are limited to linear combinations of basis functions (reflectance matrix eigenvectors), our method uses arbitrary nonlinear functions and seems more intuitive since it starts with the desired curve family properties. Relaxing the linearity requirement appears to result in more robust color sensor characterizations from spectral samples. The demonstrated neural network model yields non-negative and continuous functions of wavelength with a parameter vector for each tristimulus channel optimized based on a single error scalar summed over 10 nm wavelength intervals and IEC 61966-8 test chart sample patches.

One potential disadvantage of nonlinear optimization is the possibility of finding only one of multiple local minima in the estimation process. However, this did not seem to be a problem in practice and can be avoided by using small models and by varying the initial estimation parameters.

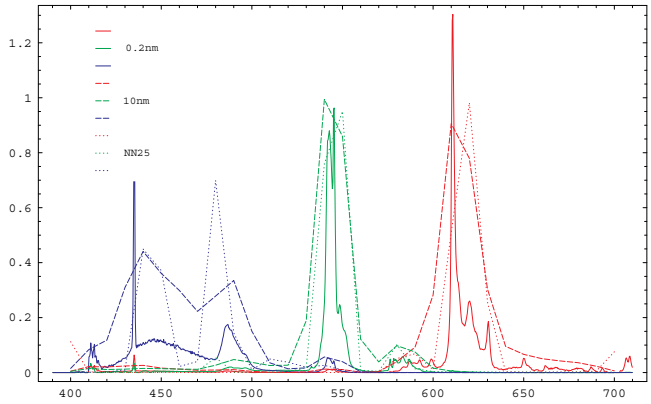

Figure 7: *Comparison of Avision AV810C scanner sensitivities. Continuous line represents the measurements having approx. 0.2 nm nominal resolution, dashed line is the result of subsampling of this data to 10 nm, and the dotted line is an estimate obtained with model* NN(25).

References

[1] G. Sharma and H. J. Trussel. Characterization of scanner sensitivity. In *Proceedings of the IS&T/SID Color Imaging Conference*, pages 103–107, November 1993.

[2] B. Dyas. Robust color sensor response characterization. In *Proceedings of the IS&T/SID Color Imaging Conference*, pages 144–148, November 2000.

[3] P. M. Hubel, D. Sherman, and J. E. Farrell. A comparison of method of sensor spectral sensitivity estimation. In *Proceedings of the IS&T/SID Color Imaging Conference*, pages 45–48, November 1994.

[4] Publication IEC 61966-8 (2001-02): Multimedia systems and equipment – Colour measurement and management – Part 8: Multimedia colour scanners, 2001.

[5] G. D. Finlayson, S. Hordley, and P. M. Hubel. Recovering device sensitivities with quadratic programming. In *Proceedings of the IS&T/SID Color Imaging Conference*, pages 90–95, November 1998.

[6] K. Barnard and B. Funt. Camera characterization for color research. *Color Research and Application*, 27(3):153–164, 2002.

[7] M. G. A. Thomson and S. Westland. Color-imager calibration by parametric fitting of sensor responses. *Color Research and Application*, 26(6):442–449, 2001.

[8] M. F. Møller. A scaled conjugate gradient algorithm for fast supervised learning. *Neural Networks*, 6:525–533, 1993.

[9] H. J. Trussell. A review of sampling effects in the processing of color signals. In *Proceedings of the IS&T/SID Color Imaging Conference*, pages 26–29, October 1994.

[10] M. J. Vrhel and H. J. Trussel. Color correction using principal components. *Color Research and Applications*, 17:328–338, 1992.

[11] K. Schittkowski. *QLD: A FORTRAN Code for Quadratic Programming, User's Guide*. Mathematisches Institut, Universität Bayreuth, Germany, 1986.

[12] G. Wyszecki and W. S. Stiles. *Color Science: Concepts and Methods, Quantitative Data and Formulae*. John Wiley and Sons, 1982.